Journal of Pharmaceutical and Biomedical Analysis 199 (2021) 114065

Contents lists available at ScienceDirect

Journal of Pharmaceutical and Biomedical Analysis

journal homepage: www.elsevier.com/locate/jpba

Polypyrrole and enzyme free cholesterol flakes based composite: Selective determination of theophylline

R. Ramya, P. Thivya, D. Nathiya, J. Wilson*

Polymer Electronics Lab, Department of Bioelectronics and Biosensors, Alagappa University, Karaikudi, 630 003, Tamil Nadu, India

ARTICLE INFO

Article history:
Received 27 October 2020
Received in revised form 31 March 2021
Accepted 2 April 2021
Available online 6 April 2021

Keywords:
Polypyrrole
Theophylline
Cholesterol
Square wave voltammetry

ABSTRACT

In the present work, we demonstrated the non-enzymatic theophylline (TP) detection using nanostructured Polypyrrole (Ppy) and Cholesterol (Ch) flakes coordinated nanocomposite coated on Glassy Carbon Electrode. The higher active surface area and good mechanical stability of the Ppy integrated Ch composite exhibited better oxidation towards TP. The electron transfer across hydrogen bonding is of fundamental importance in enhancing the biochemical process in this biosensor system. Further, the scan rate analysis confirmed the quasi-reversible diffusion controlled electrochemical process. The differential pulse voltammetry report of the electrocatalyst shows a linear response of TP in the concentration range 1 μM – 1 mM with detection limit of 720 nM (S/N = 3σ/b). The proposed electrochemical sensor exhibited intriguing sensing properties with good selectivity, reproducibility towards TP detection without any surface fouling. The overall analysis confirmed that the prepared nanocomposite modified electrode has quantified better accuracy towards target molecule without the aid of any bio receptors and binders in tea leaves and human urine samples.

1. Introduction

In recent years, conducting polymers in biosensors are profoundly explored due to their excellent biocompatibility and good conductivity observed throughout the redox process [1,2]. In the last few decades, different nanostructured CPs based composites with their interesting behaviors have received enormous attention for the construction of biosensors using the synergistic effect [3]. Polypyrrole is one of conducting polymers that demonstrated outstanding sensitivity and good versatility because of the presence of conjugated double bonds along the backbone of the polymer chain, hydrophilicity, and high electron affinities. However, the major obstacle for using Ppy based biosensors is poor adherence to electrode surface [4,5]. But this disadvantage might be overcome by doping the counter ions such as inorganic cations, anions, molecules, and the incorporation of metal oxides or new template molecules [6].

Cholesterol is an essential component of cell membrane. The conformational lengths of the side chain along with hydrophilic and lipophilic functional moieties provide intermolecular contacts with biological molecules [7]. For example, different lipids were synthesized, based on Ch for drug delivery application and also experimental results indicated the copolymer with Ch established self-assembly with excellent fluorescence behaviour [8]. Recently, Ch demonstrated good bio-functionalization ability with cyclodextrin and Ch based derivatives exhibited the highest antibacterial activity against *E. coli* with moderate antifungal activity against *C. albicans* and *A. flavus* [9]. According to recent studies, the self assembly nature and biocompatibility of Ch with polymers observed potential application in anticancer, drug delivery, genomics and no in biosensor. However, no reports so far using Ch based composite for the fabrication of TP biosensor. In this work, the physiological molecule Ch is used for surface modification and the protective hydrophobic layer over the surface of Ppy cationic polymer provides enhanced stability. Also, Ch forms integrity by successful linkage of hydroxyl group with amine in polypyrrole. The prepared eco-friendly Ch based nanocomposite exhibited preferred bio-adhesion by a special biophysical mechanism for the effective enzyme free TP sensing.

Theophylline (TP) is one of the most clinically monitored, methylated derivatives of xanthine, used in respiratory stimulators for the treatment of acute and chronic asthmatic conditions [10]. The useful plasma level of TPs for the effective bronchodilation action is 20–100 μM concentration range and beyond this the drug becomes toxic causing tachycardia, nausea, arrhythmia, and

* Corresponding author.
E-mail address: wilson.j2008@yahoo.com (W. J.).

https://doi.org/10.1016/j.jpba.2021.114065
0731-7085/

convulsions [11]. So, the TP's narrow therapeutic index needs alert observation to restrict its toxic side effects.

Xiaolin Cuia et al., demonstrated TP detection using Surface-Enhanced Raman Spectroscopy technique which holds advantages of increased sensitivity and simultaneous detection of analytes. But limited reusability, degradation of analytes along with time and limited selectivity restricts it applicability [12]. RNA aptamers based composite with resins for TP detection based on single molecule photo bleaching technique was investigated by Shi Gang Liu et al. This route excellently provides high sensitivity, but problems arises with high-end instrumentation along with numerous steps and loss of fluorescence after bleaching makes this one complicated [13]. Similarly, Yuan-Ting Li et al., used MIP-SERS nanoprobe for the TP detection, which deals the same complications in reusability, selectivity and degradation making a demand for eliminating the errors [14]. Lucia Bartella et al., proposed fast screening of caffeine, theobromine and TP based on Tandem Mass Spectrometry and PS-MS analysis. Although this protocol produces accurate results with high precision and selectivity, this method lacks in pre-sample preparation, using of organic solvents, high operational cost with limited sample throughput and less favorable sample concentration [15]. On the other hand, electrochemical technique is found attractive due its cost and simplicity recently. Yingchun Duan et al., demonstrated a novel electrochemical sensor for quantifying TP by electro spinning process which comprises complex steps [16]. Similarly, Rwaida et al., used tert-Butyl calixarene tetra kis(N, N-dimethylacetamide) as a sensing ionophore in the presence of MWCNTs-CuO nanohybrid. However, in the above said electrochemical route the materials itself will limit its application because they involve toxic solvents making this as non-ecofriendly sensing platform for TP detection [17].

In this work, we have demonstrated enzyme free biosensor by a facile polymerization route without involving any cross linker, initiator tedious instrumentation, high temperatures, toxic chemicals.The aim of this work is to explore the electrochemical performance of this new composite by synergetic effect and exhibited high sensitive biosensor.The performance of the bioelectrode system was also evaluated to the quantification of TP in a human urine sample and tea leaves with satisfactory results, as shown in scheme 1 .

2. Experimental section

2.1. Reagents and materials

All chemicals were of analytical grade. The purity/assay of all chemicals are: Polypyrrole and Ch- 98 %, Thiouria- 99.0 %, Xanthine, Caffiene, dyphylline, theobromine, methyl orange, Ferric chloride- 98 %, theophylline- 98.0 %, sodium dihydrogen phosphate 98 %, disodium hydrogen phosphate 99.0–100.50 % and were purchased from Sisco Research Laboratories. TP- 98 % was received from Alfa Aesar. 0.1 M phosphate buffer solution (PBS) with different pH values was prepared by mixing the stock solutions of NaH_2PO_4- 98.0 % and Na_2HPO_4- 99.0- 100. 50 % and then TP was freshly prepared using PBS. All the solutions were prepared with ultra pure water from a Millipore system. Glassy Carbon Electrodes (GCE) working electrodes procured from Zensor Technologies, India.

2.2. Instruments and measurements

The electrochemical behaviour of prepared samples was studied using a Biologic SP-150 electro-chemical work station (France). The three electrode system consisting of working glassy carbon electrode (0.07 cm^{-2}), Ag/AgCl (3.0 M KCl) reference electrode and platinum wire auxiliary electrode in a electrochemical cell, filled with 10 mL of PBS at room temperature. During the CV and EIS measurements, the electrolyte solution was constantly kept with nitrogen atmosphere in a background solution of 1 mM $[Fe(CN)_6]^{3-/4-}$ in 0.1 M KCl at 50 mVs^{-1} scan rate and recorded in the frequency region 100 kHz to 1 Hz at an applied DC potential 230 mV and amplitude of ±5 mV. The Raman spectra were carried out, in air at room temperature by laser Raman spectrometer (model STR 500 mm focal length, SEKI Japan). Powder X-ray diffraction (XRD) analysis was performed on a Bruker Germany D8 instrument. UV analysis was performed with a Shimadzu UV-1700 photometer. The functional groups of the prepared samples were identified from Fourier transform Infrared (FT-IR) spectra recorded by Thermo Nicolect 380 instrument. The morphology of the samples was checked by scanning electron microscopy (SEM) and Energy-dispersive X-ray spectroscopy (EDS) was analyzed using Carl Zeiss EVO 18 instrument.

2.3. Polypyrrole nanospheres synthesis

The typical synthesis of the preparation of Ppy is as follows. Briefly, 0.5 g $FeCl_3$ was mixed with 5 mM methyl orange solution (60 mL) and vigorous stirring for 30 min. Subsequently, 210 µl pyrrole monomer was added drop by drop for 10 min and left under static condition for 36 h at −5 °C. The obtained black precipitate was filtered, then washed with de-ionized (DI) water, ethanol and dried in a vacuum oven for 12 h at 45 °C. Then the optimized amount of 0.2 g Ch and 0.3 g Ppy was taken in eppendorf tube, added 1 mL DI water and sonicated for 3 h. Then the mixture was used for the electrochemical studies.

2.4. Tea sample

The practical application of the Ppy-Ch modified electrode was tested by measuring the concentration of TP in tea leaves. The exactly weighed 50 mg of tea leaves was added with DI water in a 50 mL of beaker, stirred with heat to 80 °C for 15 min. Then the tea sample was filtered and cooled to room temperature. Finally, the sample was diluted to 50 mL by DI water for the detection of TP.

2.5. Human urine sample

The human urine sample was collected from healthy female and diluted by 10 times using pH 7.0 PBS. Then, 100 µl diluted urine sample was added to 20 mL PBS and used for the electrochemical studies.

3. Results and discussion

3.1. Structural analysis

3.1.1. XRD analysis

The comparative crystal structure characterization of Ppy, Ch, Ppy-Ch hybrid material was performed by XRD, as depicted in Fig. 1A. The diffracted peak of Ppy around 25° can be assigned to amorphicity, which indicates short range arrangement chain [18]. The average size of the Ppy microsphres was estimated to be 58 nm using the Scherrer formula. The multiple characteristic peaks with different intensities of Ch flakes exhibited triclinic structure with broad peak at12°, 14°,15°,16° [19,20] which are in good concord with JCPDS data [07−0742]. The phase and structural change of the hybrid sample were well observed and further the peak shift along with intensity variation also supports the composite formation. In the composite the semi-crystallinity is not only improved the con-

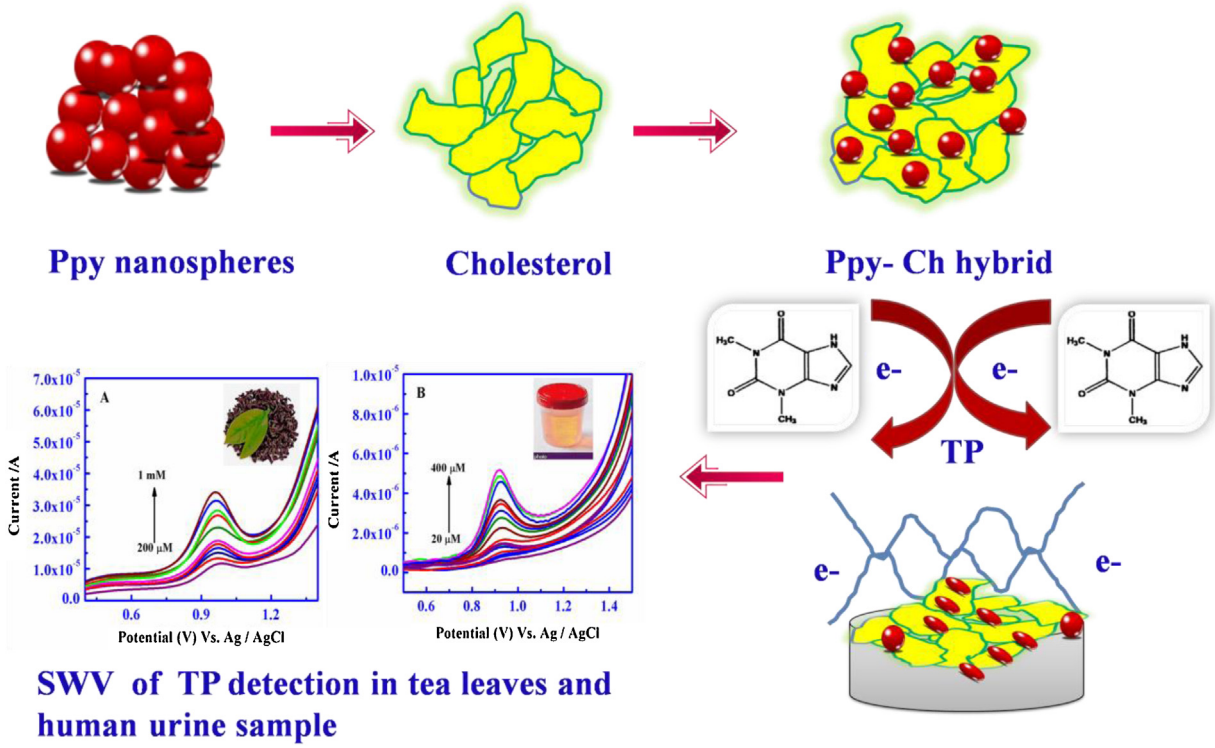

Scheme 1. Illustration of preparation of Ppy-Ch hybrid structure for TP detection.

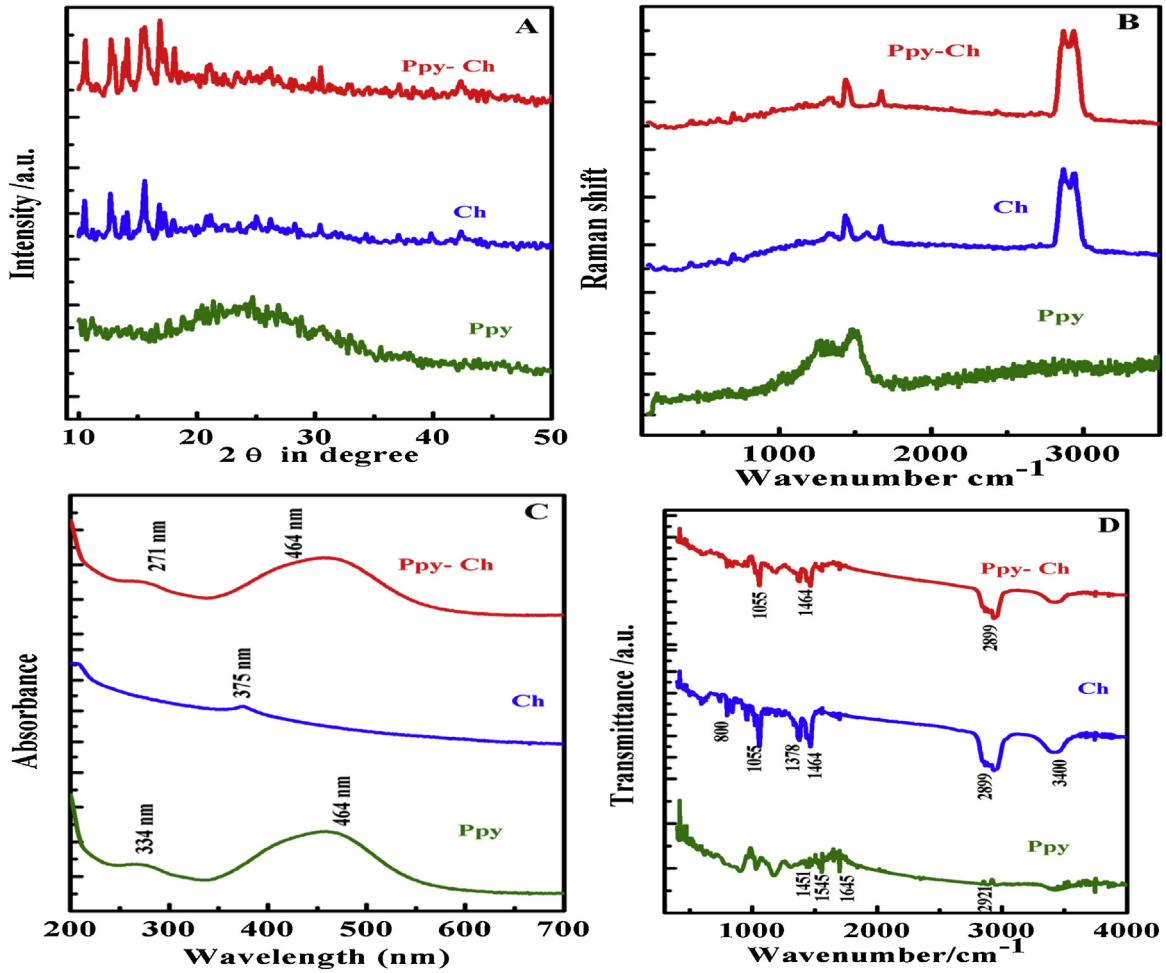

Fig. 1. (A) XRD patterns (B) Raman spectra (C) UV patterns (D) FTIR spectra of Ppy, Ch, Ppy-Ch hybrid structure in PBS (pH 7).

ductivity but also mechanical stability enhanced which is useful for efficient detection of TP [21].

3.1.2. Raman study

The Raman scattering study was performed by inelastic collision of photons to detect new chemical bonds formed in the hybrid materials, shown in Fig.1B. The pure Ppy depicts an important peak at 1589 cm^{-1} which can be ascribed to C═C backbone stretching, and the peak at 1393 cm^{-1} further support the stretching mode of polymeric material [22]. The Raman spectrum of pure Ch with sharp peak in the spectrum found at 2906 cm^{-1} due to the C—H stretching modes with additional peaks at 1680 cm^{-1}, C═C stretching modes and at 1440 cm^{-1} the CH_2 scissoring mode respectively [23]. In the Ppy-Ch hybrid, the intensity variation and peaks of Ch shift in composite confirms the composite formation.

3.1.3. UV study

The UV- absorption spectroscopy study of Ppy, Ch and Ppy-Ch hybrid samples was examined and as shown in Fig.1 (C). A distinct weak spectra at 334 nm and broad shoulder at 464 nm, could be interpreted to π^*-π transition of Ppy [24]. And then, the small absorption peak around 207 nm represents the —C═C— band supporting the presence of Ch [25]. Also, the —C═C— bands attached to one or two tertiary carbon atoms, as a result absorbance around 334–375 nm, informing successful preparation of Ppy-Ch composite.

3.1.4. FTIR spectra

The IR spectroscopy gives a 'fingerprint' of substance with respect to their molecular formation. The FTIR spectral analysis was carried out to confirm the chemical bonds and functional groups present in the samples (Fig. 1D). The peaks at 1545 cm^{-1} and 1451 cm^{-1} as a result of C—N and C—C stretching while the peaks centered at 2921 cm^{-1} and 1645 cm^{-1} accredited to C—H stretch vibration indicate the presence of the Ppy backbone chain [26,27]. The observed wave number for C—H out-of-plane bending mode at 800 cm^{-1} and the sharp peak at 1055 cm^{-1} can be attributable to ring deformation of Ch. The weak peak at 1378 cm^{-1} is credited to the CH_2 and CH_3 bending vibration of Ch and 1464 cm^{-1} due to asymmetric stretching. The hydrogen bond formation as a result of electrostatic interaction is responsible for the shift in characteristic peak at 2899 cm^{-1} and further the observed broad and intense band (Fig. 1D) nearly at 3400 cm^{-1} confirming the composite formation [28].

3.2. Morphology analysis

Morphology of the prepared samples is summarized in SEM images shown in Fig. 2. In the inset Fig.2A displays slightly agglomerated the morphology of Ppy microspheres and its size is calculated using Dynamic Light Scattering technique as 1.9 μm. The micrograph of Ch flakes is seen with irregular size in Fig. 2B. This flake structure may actually be useful to binding with Ppy via H_2 bonding. Fig. 2C shows the Ppy microspheres surrounded to the Ch surface which could increase specific surface area and provide more binding sites for analyte interaction. As a result, better electron conductivity and electrocatalytic activity for the detection of TP is witnessed. EDS spectrum for elemental analysis of Ppy-Ch hybrid formed are of C- 85.9 %, O- 13.9 % and Cl- 0.3 % and shown in Fig.2D.

3.3. Electrochemical characterization

3.3.1. CV behaviour of the Ppy-Ch hybrid structure in $[Fe(CN)_6]^{3-/4-}$ solution

CV analysis was performed to explore the stepwise modification of electrodes in a solution containing 1 mM $K_3Fe(CN)_6/K_4Fe(CN)_6$ (1:1) and 0.1 M KCl to monitor the redox behaviour of electroactive species over a wide potential range (Fig. 3(A)). The CV at the bare GCE (18.85 μA) shows a well defined couple of redox peaks by the ferricyanide ion. After the electrode modification with Ppy (33.71 μA), the curve changed drastically. As seen in Ch-GCE, when the Ch was drop casted on the electrode surface, a decrease in peak current was recorded indicating that the Ch sample had partially blocked the electron transfer. Interestingly at the Ppy-Ch/GCE due to larger curve area, a well improved charge transport process responses with high current (47.69 μA).This happens because of successful electrostatic interaction between positively charged Ppy with negatively charged Ch and faster charge transfer rates favorable for rapid diffusion of electrons by providing a low diffusion length. Further, the electrochemical active surface area of different materials such as bare, Ppy, Ch and Ppy-Ch modified electrodes is also calculated by using Brown-Anson model formula and their values: 3.9 nmol/cm^2, 6.05 nmol/cm^2, 2.54 nmol/cm^2, 7.54 nmol/cm^2 respectively and these results supports maximum surface area of the composite helps for good redox process in ferrocyanide solution.

The stepwise assembly of the bioelectrode was monitored to study the interfacial properties of the electrode surface using EIS, Fig. 3(B). From high frequency semicircle, the value of R_{ct} at the electrode surface was calculated. The impedance curve of the bare GCE shows 96 Ω with a small semicircle representing the diffusional limiting step. As shown in curve b, with increased in semicircular diameter depicts 720 Ω for Ppy. The very large semicircle was observed for deposition of Ch (curve c) indicating successful coating on the electrode in which the electron transfer was hindered by the ferrocyanide solution to reach the electrode surface. Also, the blocking and polarization of electron transfer is responsible for high resistance [29]. On the other hand, in the Ch-Ppy composite, the diameter of the high frequency semicircle was significantly decreased with a lowest R_{ct} value of 86 Ω (curve d), implying that Ch may play an important role by maintaining its crystallinity and accelerated the electron transfer rate. The EIS results confirmed different layers formation on the electrode surface and found consistent with that of CV analysis, thus validating the successful fabrication of the Ppy-Ch/GCE. [30].

The blank CV investigation of Ppy/GCE and Ppy-Ch/GCE modified electrodes in 0.1 M KCl containing 1 mM $Fe(CN)_6^{-3/-4}$ at different scan rates 10–100 mV/s was performed, Fig.S1 A.B. A subsequent increased in redox peak currents was observed with increasing scan rate value for both electrodes and also the peak currents are proportional to the square root of the scan rate (inset of Fig.S1) informing diffusion controlled electron transfer process. It is very well observed that the slope of the hybrid Ppy-Ch sample is steeper confirming better electrocatalytic activity.

3.3.2. Electrocatalytic oxidation of TP

The electron transfer behaviour of different modified electrodes was investigated using CV method in PBS. No significant redox peaks for TP were noticed in the modified electrodes except Ppy-Ch/GCE surface as seen in Fig. 3C. i.e. the oxidation of TP in PBS shows a well-defined oxidation peak at 1.089 V for Ppy-Ch/GCE. The oxidation peak can be attributed to electro-catalytic activity of Ch with Ppy modified electrode by enhancing the electron transfer process and also the composite plays a suitable mediator role to shuttle electron between modified surface and redox probe. This phenomenon might be caused by the fast electron transfer in the

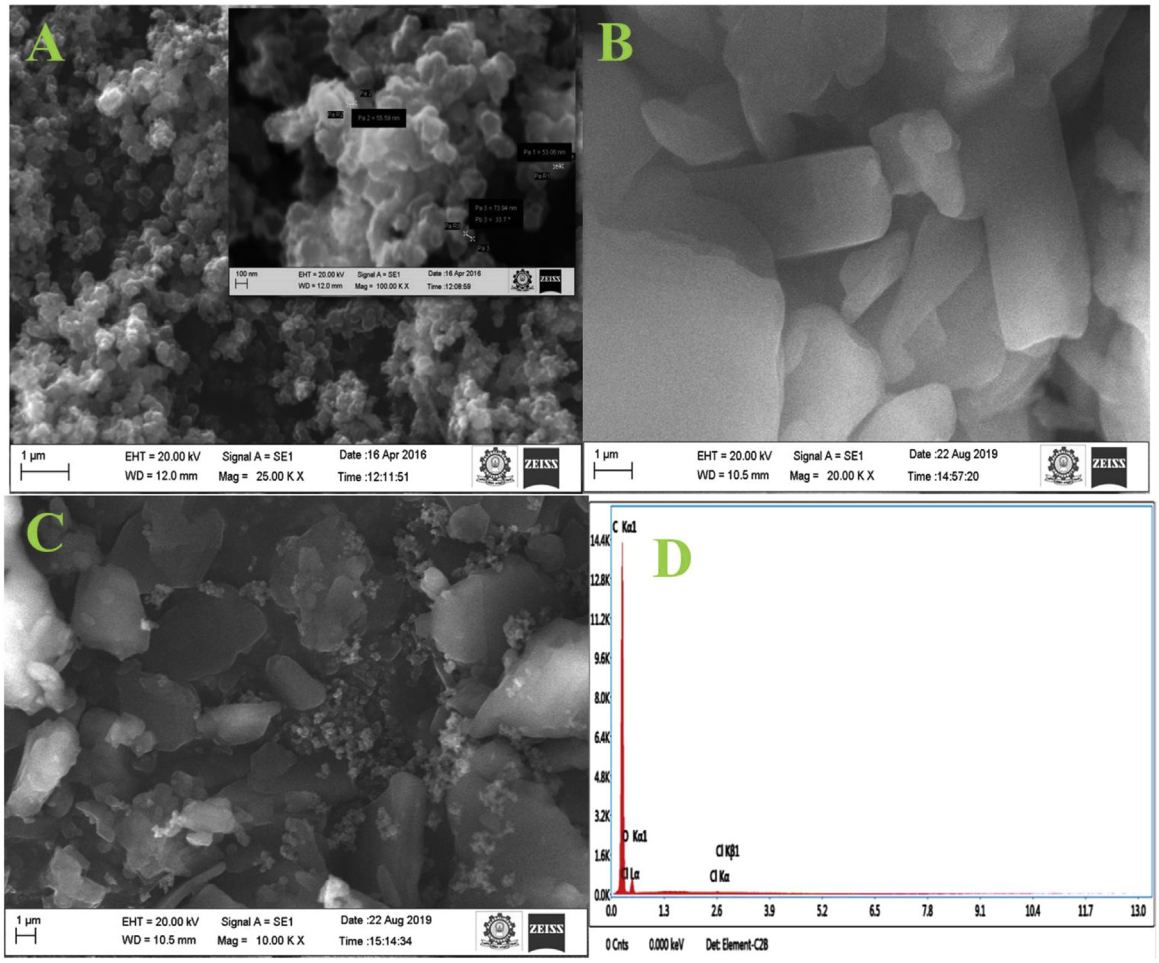

Fig. 2. SEM images of (A) Ppy nanospheres (B) Ch flakes (C) Ppy-Ch hybrid and (D)EDS spectrum of hybrid structure.

compact structure by the amine group of Ppy and hydroxyl group of Ch in the composite with amine, O and N groups of TP.

The linear relationship between oxidation peak current (i_{pc}) and scan rate$^{1/2}$ is shown in (Fig. S2). The oxidation peak current increased gradually with increase of scan rate. In the scan rate range 10 mV–90 mV s^{-1} the linear relationship was established between I_p and v, which can be expressed as: I_p (μA) 0.637 mV s^{-1} + 20.24 (R = 0.995), and indicated that the oxidation of TP on Ppy-Ch surface was diffusion controlled, as shown in Fig. S1B. The selection of correct pH value has great influence on the biosensor fabrication. So the pH range 3.0–9.0 at the Ppy/Ch GCE was investigated on the anodic peak current and potential of TP in PBS, by CV. The peak currents of TP increased with increasing solution pH until it reached about 7.0, beyond the current decreased with the further increase in pH. Based on these results, the peak currents are strongly dependent on pH signaturing the participation of H^+ ions in the oxidation of TP. As seen in Fig. 3(D), the H^+ in the oxidation process of Ppy/Ch system generates the maximum current response at pH 7 and gradually decreases its catalytic activity when the pH is increased to base values. Based on these physiological results, pH 7 is optimized for further investigation.

3.4. SWV of TP determination

To examine the demonstrable efficiency of the proposed Ppy/Ch based biosensor, a sensitivity analysis was explored via SWV measurements at various concentrations of the TP. As illustrated in Fig.4A, the oxidation peak potential was at 1.02 V and the peak current of analyte increased linearly from 6.55 μA to 47.59 μA. The corresponding different TP concentrations versus oxidation currents, as shown in Fig.4B, demonstrates a good linear relationship over a range of 1 μM – 1 mM with the detection limit 720 nM (S/N = 3σ/b), and their regression coefficient was 0.997. The equivalent regression equation is y = 0.0399x + 7.7046. It is obvious that the method is quite sensitive and can be concluded that the present modified electrode shows the lower detection limit towards TP, demonstrating that the Ppy/Ch/GCE hybrid is a good alternative for the determination of TP. Furthermore, this Ppy-Ch/GCE electrochemical system explores a simple route as compared to using complex multistep construction and costly enzymes (Table S3).

3.5. Reproducibility and stability of sensors

A freshly prepared biosensor was subjected to monitor the variation in its current response towards TP as a function of time and the number of readings for a period of 7 h, 15 CV measurements of 200 μM TP 0.1 M PBS. The experimental results demonstrated that the bioelectrode retained 75 % of its initial value after15 measurements. Further, the storage stability of the biosensor was verified by calculating the change in its current response for a 200 μM TP solution at regular interval of 1 week for about 1 month, stored at 4 °C in PBS when not in use. It has been found that the bioelectrode retained 93 % of its initial response after 1 month. The reproducible behaviour of the biosensor was performed from the response to 200 μM TP at 5 electrodes prepared by uniform procedure. The biosensor demonstrated good reproducibility with a RSD of 5.4 %,

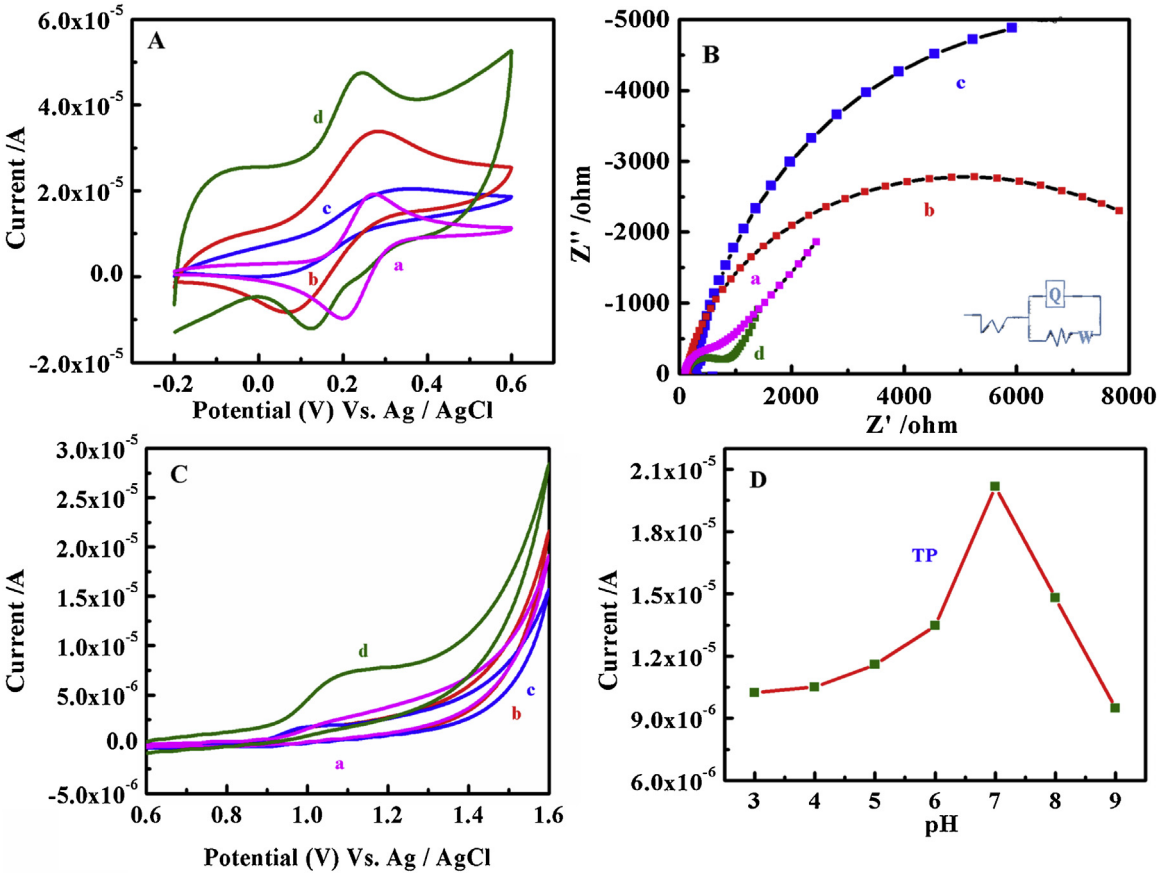

Fig. 3. (A) CV (B) EIS Profiles: (a) bare/GCE (b) Ppy/GCE (c) Ch/GCE (d) Ppy-Ch/GCE modified electrodes at 50 mVs^{-1} in 1 mM of $[Fe(CN)_6]^{-3-4}$ and 0.1 M of KCl. (C) Ppy-Ch/GCE hybrid in 200 μM TP at 50 mVs^{-1} (D) pH versus current.

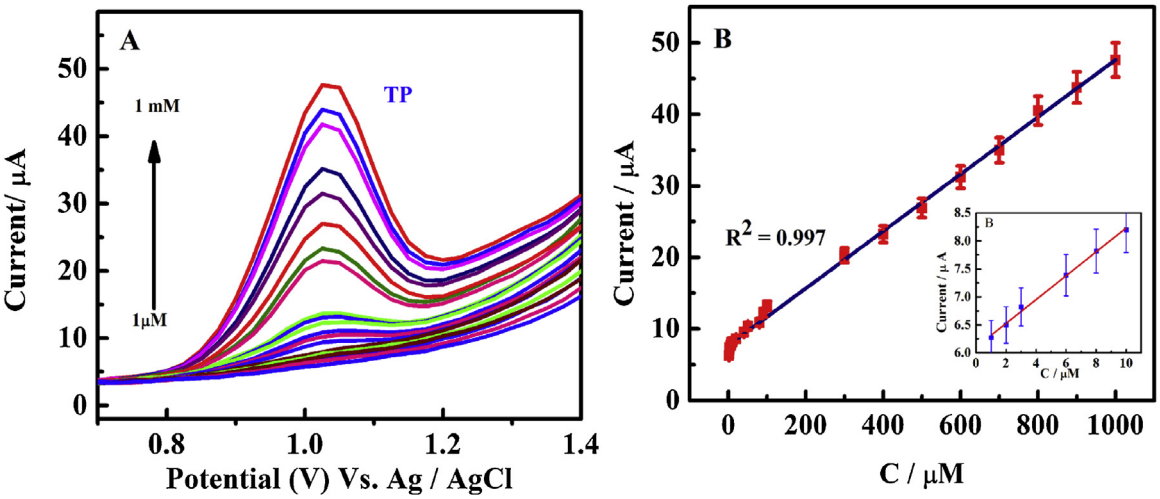

Fig. 4. SWV profiles (A) 1 μM–1 mM TP (B) plot of the oxidation peak current against concentration of TP at Ppy/Ch hybrid GCE in 0.1 M PBS (pH 7.0).

as seen in Fig. S6(B). Also, the working stability of the Ppy/Ch/GCE was investigated by continuous 100 cycles in presence of 200 μM TP (Fig. S4A). These results indicate that the proposed biosensor has a good stability and does not undergo any surface entangling.

3.6. Analytical applications

To explore the selectivity of the biosensor towards TP, the effect of some interfering compounds with 100 fold concentration such as xanthine, caffeine, dyphylline, theobromine using amperometry study was demonstrated in presence of PBS, pH 7, containing 100 μM TP, Fig. S4 (B&C). Further, the selectivity coefficient (SC) of the fabricated bioelectrode for each interferent was calculated using the formula, SC = Ic + i/Ic where Ic + i and Ic are bioelectrode response at 1.01 V for TP (100 μM) in the presence and absence of each interferents, respectively. The results indicate that response of bioelectrode did not significantly affect the current value by the presence of these interferents (Fig. S4). These results show no

remarkable interaction with interferents and also the fabricated biosensor had good anti-interference ability (Fig. S3; S.Table1). The fresh tea and normal human urine samples were identified with the Ppy/Ch/GCE biosensor to monitor its usage for real samples. Standard addition technique was chosen to quantify the TP content in them. From the tea sample with known concentrations (200 μM-1 mM), the TP values were calculated using the response current, shown in Fig. S5(A). Similarly, for urine sample of different concentrations (20–400 μM), the TP values were recorded, Fig. S5(B). As summarized in Table S2, the % recovery values for the spiked samples inform the reliability of the proposed biosensor and its effectiveness towards TP analysis in clinical detection.

4. Conclusions

We have fabricated an enzyme free electro chemical biosensor based on Ppy and Ch based biocomposite for TP detection. The hydroxyl groups of Ch developed the electrostatic interaction and enriched the stability, thus crystallinity of the composite was well improved in quantifying the TP. The simple developed biosensor demonstrates an excellent electrochemical oxidation of TP by bioadhesive nature of Ch. The biofunctionalized material explored theTP determination of in real samples with satisfactory results. Therefore, considering the real time application of the designed bioelectrode, the proposed sensor might be used in food sensor and pharmaceutical field in future.

CRediT authorship contribution statement

R. Ramya: Conceptualized, investigated and planned the work along with methodology and writing the original draft. **P. Thivya:** validated the results and interpreted the data. **D. Nathiya:** reviewed the writing and did formal analysis along with validation. **Dr. J. Wilson:** the corresponding author administrated and supervised the project, arranged the needed resources and investigated the final results.

Declaration of Competing Interest

The authors declare that they have no known competing financial interests or personal relationships that could have appeared to influence the work reported in this paper.

Acknowledgements

The author J.W. gratefully acknowledges the University Grant Commission (MRP-MAJOR-ELEC-2013-37628) for financial assistance and RUSA 2.0[F.24-51/2014-U,Policy (TN Multi-Gen), Dept.of.Edn,Gol].

Appendix A. Supplementary data

Supplementary material related to this article can be found, in the online version, at doi:https://doi.org/10.1016/j.jpba.2021.114065.

References

[1] R.A. Green, N.H. Lovell, G.G. Wallace, L.A. Poole, Warren, Conducting polymers for neural interfaces: challenges in developing an effective long-term implant, Biomaterials 29 (2008) 24–25.
[2] A. Ramanaviciene, A. Kausaite, S. Tautkus, A. Ramanavicius, Biocompatibility of polypyrrole particles: an in-vivo study in mice, J. Pharm. Pharmacol. 59 (2007) 311–315.
[3] B. Garner, A.J. Hodgson, L. Liu, G.G. Wallace, Polypyrrole–heparin composites as stimulus-responsive substrates for endothelial cell growth, J. Biomed. Mater. Res. 44 (1999) 121–129.
[4] N.K. Guimard, N. Gomez, C.E. Schmidt, Conducting polymers in biomedical engineering, Prog. Polym. Sci. 32 (32) (2007) 8–9.
[5] K.E. Hnida, R.P. Socha, G.D. Sulka, Polypyrrole-silver composite nanowire arrays by cathodic co-deposition and their electrochemical properties, J. Phys. Chem. C. 117 (2013) 19382–19392.
[6] M. Brust, M. Walker, D. Bethel, l.D.J. Shifrin, R. Whyman, Synthesis of thiol – derivatized gold nanoparticles in a 2- Phase liquid-liquid system, J. Chem. Soc., Chem.Commun. (1994) 801–802.
[7] N.B. Mayant, Medical Books, Willium Heinemann, London, 1981.
[8] O. Kleiner, J. Ramesh, M. Huleihel, B. Cohen, K. Kantarovich, C. Levi, B. Polyak, R.S. Marks, J. Mordehai, Z. Cohen, S. Mordechai, A comparative study of gallstones from children and adults using FTIR spectroscopy and fluorescence microscopy, BMC Gastroenterol. 2 (2002) 1–14.
[9] F. Reinitzer, Contributions to the knowledge of cholesterol, Monatsh. Chem. 9 (1888) 421–441.
[10] L. Hendeles, M. Weinberger, G. Johnson, Monitoring serum theophylline levels, Clin. Pharmacokinet. 3 (1978) 294–312.
[11] D.R. Sliskovic, A.D. White, Therapeutic potential of ACAT inhibitors as lipid lowering and anti-atherosclerotic agents, Trends Pharmacol. Sci. 12 (1991) 194–199.
[12] Xiaolin Cuia, Menghua Songc, Yan Liua, Yifan Yuana, Qiang Huangc, Yongbing Caob, Feng Lu, Identifying conformational changes of aptamer binding to theophylline: A combined biolayer interferometry, surface-enhanced Raman spectroscopy, and molecular dynamics study, Talanta 217 (2020), 121073.
[13] Shi Gang Liu, Dong Zhang, He Yu, Wenli Gao, Xingbo Shi, A split aptamer sensing platform for highly sensitive detection of theophylline based on dual-color florescence colocalization and single molecule photobleaching, Biosens. Bioelectron. 166 (2020), 112461.
[14] Yuan-Ting Li, Yuan-Yuan Yang, Ying-Xin Sun, Yue Cao, Yan-Shan Huang, Sheng Han, Electrochemical fabrication of reduced MoS2-based portable molecular imprinting nanoprobe for selective SERS determination of theophylline, Microchim. Ichnoanal. Acta 4 (2020) 4201–4203.
[15] Lucia Bartella, Leonardo Di Donna, Anna Napoli, Carlo Siciliano, Giovanni Sindona, Fabio Mazzotti, A Rapid method for the assay of methylxanthines alkaloids: theobromine, theophylline and caffeine, in cocoa products and drugs by paper spray tandem mass spectrometry, Food Chem. 278 (2019) 261–266.
[16] Yingchun Duan, Anqing Wang, Yaping Ding, Li. Li, Jiaxin Lin DingdingDuan, Chenhong Yu, Jiayifan Liu, Fabrication of poly-sulfosalicylic acid film decorated pure carbon fiber as electrochemical sensing platform for detection of theophylline, J. Pharm. Biomed. Anal. 192 (2021), 113663.
[17] A.Rwaida Al-Haidaria, A.Nehad Abdallaha, M.Mai Al-Oqailc, S.Ebtesam Al-Sheddic, M.Shaza Al-Massaranic, N.Nida Farshoric, Nanoparticles based solid contact potentiometric sensor for the determination of theophylline in different types of tea extract, Inorg. Chem. Commun. 119 (2020), 108080.
[18] B.D. Cullity, Elements of X-Ray Diffraction, Addison-Wesley Publishing Company Inc, London, 1978.
[19] H.S. Sheih, L.G. Hoard, C.F. Nordman, The structure of cholesterol, Acta Cryst. B. 37 (1978) 1538–1543.
[20] B.M. Craven, Pseudosymmetry in cholesterol monohydrate, Acta Cryst, B. 35 (1979) 1123–1128.
[21] Erin M. Sullivan, Oh Yun Ju, Rosario A. Gerhardt, Ben Wang, Kyriaki Kalaitzidou, Understanding the effect of polymer crystallinity on the electrical conductivity of exfoliated graphite nanoplatelet/polylactic acid composite films, J. Polym. Res. 21 (2014) 563.
[22] M. Poorvesh, J. Vyas1 Mihir, Joshi, Surface Micro topographical and dielectric studies of cholesterol crystals, Adv. Mat. Res. 665 (2013) 289–296.
[23] S. Sakthivel, A.J. Boopathi, Chem. Chml. Sci. 4 (2014) 150–155.
[24] G. Alba Alfonso-García Simon Pfisterer, Howard Riezman, Elina Ikonen, O. Eric, A. Potm, D38-cholesterol as a Raman active probe for imaging intracellular cholesterol storage, J. Biomed. Opt. 21 (2006) 6–8.
[25] B. Yeole, T. Sen, D.P. Hansora, S. Mishra, J. Appl. Polym. Sci. Symp. 132 (2015) 423–429.
[26] Rodriguez, Rabid analysis of oxyterols by HPLC and uv spectroscopy, BioTechniques 36 (2004) 952.
[27] R. Ramya, P. Muthukumaran, J. Wilson, Electron beam-irradiated Polypyrrole decoratedwith Bovine serum albumin pores: simultaneous determination of Epinephrine and L-Tyrosine, Biosens. Bioelectron. Biosens. Bioelectron. 108 (2008) 53–61.
[28] G. Liu, D. Xing, H. Yang, J. Wu, Vibrational spectroscopic study of human pigment gallstones and their insoluble materials, J. Mol. Struct. 616 (2002) 187–191.
[29] X.S. Zhou, G.R. Shen, J.G. Wu, Aspectroscopic study of pigment gallstones in china, Biospectroscopy 3 (1997) 371.
[30] N.V. Prasad, G. Prasad, T. Bhimasankaran, S.V. Suryanarayana, G.S. Kumar, Dielectric properties of cobalt doped cadmium oxalate crystals Ind, J. Pure Appl. Phy. 34 (1996) 639–643.